Journal of Computational Mathematics
Vol.35, No.6, 2017, 801–813.

http://www.global-sci.org/jcm
doi:10.4208/jcm.1612-m2016-0677

EXPONENTIALLY FITTED TRAPEZOIDAL SCHEME FOR A STOCHASTIC OSCILLATOR*

Xiuling Yin
School of Mathematics and Statistics, Huazhong University of Science and Technology, Wuhan 430074, China
School of Mathematical Sciences, Dezhou University, Dezhou 253023, China
Email: yinxiuling@dzu.edu.cn
Chengjian Zhang
School of Mathematics and Statistics, Huazhong University of Science and Technology, Wuhan 430074, China
Email: cjzhang@mail.hust.edu.cn
Yanqin Liu
School of Mathematical Sciences, Dezhou University, Dezhou 253023, China
Email: liuyanqin_2001@163.com

Abstract

This paper applies exponentially fitted trapezoidal scheme to a stochastic oscillator. The scheme is convergent with mean-square order 1 and symplectic. Its numerical solution oscillates and the second moment increases linearly with time. The numerical example verifies the analysis of the scheme.

Mathematics subject classification: 60H10, 65P10.
Key words: Exponentially fitted trapezoidal scheme, Symplectic; mean-square order, Second moment.

1. Introduction

Stochastic oscillators are important mathematical models to evaluate the advantages and disadvantages of numerical schemes ([1–4]). Many papers discuss the linear stochastic oscillator $\ddot{u}(t) + u(t) = \lambda \dot{W}(t)$, equivalently,

$$\begin{cases} du(t) = v(t)dt, \\ dv(t) = -u(t)dt + \lambda dW(t), \\ u(0) = 1, \quad v(0) = 0, \end{cases} \tag{1.1}$$

where λ is given and $W(t)$ is Brownian motion.

Proposition 1.1. ([3,4]) *The Hamiltonian stochastic system* (1.1) *preserves the symplectic* 2-*form* $du(t) \wedge dv(t)$. *Its solution can be expressed as*

$$u(t) = \cos(t) + \lambda \int_0^t \sin(t-s)dW(s), \tag{1.2a}$$

$$v(t) = -\sin(t) + \lambda \int_0^t \cos(t-s)dW(s). \tag{1.2b}$$

* Received June 18, 2016 / Revised version received October 15, 2016 / Accepted December 20, 2016 / Published online September 13, 2017 /

$u(t)$ oscillates with infinitely many simple zeros. Moreover, it satisfies that

$$E(u(t)^2 + v(t)^2) = 1 + \lambda^2 t.$$

The proposition above tells us the solution phase flow of (1.1) is symplectic, its second moment grows linearly with time and its solution oscillates. Many papers discuss the symplectic and multi-symplectic schemes ([5–10]). The references show that numerical preservation of symplectic structure is as important as high accuracy for numerical solutions to Hamiltonian systems. Symplectic schemes can simulate stably the main qualitative property of solutions of Hamiltonian systems for long time.

Recently, exponentially fitted schemes are popular to solve ODE systems with oscillating solutions ([11–14]). They can be derived by generalizing the Runge-Kutta methods and choosing the coefficients in order to integrate exactly all functions in a selected linear space and minimize the local error of the numerical solution. [11] proposes exponentially fitted Runge-Kutta methods with s stages and introduces how to estimate the parameter. An explicit exponentially fitted Runge-Kutta method with an optimal parameter is presented in [12]. Exponentially fitted Runge-Kutta-Nyström method is constructed for second order ODE systems with oscillating solutions [13]. [14] studies two kinds of exponentially fitted Runge-Kutta methods with fixed points and with frequency-dependent points. For Hamiltonian systems, exponentially fitted schemes with structure preservation properties are proposed in [15, 16, 17, 18]. [17] proposes a fourth-order symplectic exponentially fitted scheme with modified Gauss method. [18] considers linear and quadratic discrete invariants of exponentially fitted Runge-Kutta methods.

In [4], the predictor-corrector methods are applied to the stochastic oscillator system (1.1). This work inspires us some idea. How does exponentially fitted scheme behave for the stochastic oscillator system (1.1)? Whether is the numerical solution symplectic and oscillatory? Whether does the numerical second moment grow linearly with time? In this paper we try to study and answer the question.

2. Exponentially Fitted Trapezoidal Scheme

Two stage exponentially fitted Runge-Kutta scheme with symmetric nodes applied to deterministic first-order system $y' = f(x, y)$ yields that

$$\begin{aligned} y_1 &= \gamma_0 y_0 + h(b_1 f(x_0 + c_1 h, Y_1) + b_2 f(x_0 + c_2 h, Y_2)), \\ Y_1 &= \gamma_1 y_0 + h(a_{11} f(x_0 + c_1 h, Y_1) + a_{12} f(x_0 + c_2 h, Y_2)), \\ Y_2 &= \gamma_2 y_0 + h(a_{21} f(x_0 + c_1 h, Y_1) + a_{22} f(x_0 + c_2 h, Y_2)). \end{aligned} \tag{2.1}$$

Here $c_1 = 1/2 - d, c_2 = 1/2 + d$. To make the scheme exact for the linear fitting trigonometric space generated by $\{1, exp(\pm i\omega x)\}$ and symplectic [18], we get exponentially fitted trapezoidal scheme with $d = 1/2, \gamma_0 = \gamma_1 = \gamma_2 = 1, a_{11} = a_{12} = 0, a_{21} = a_{22} = b_1 = b_2 = \frac{1-\cos(\omega h)}{\omega h \sin(\omega h)}$, equivalently,

$$y_1 = y_0 + \frac{1 - \cos(\omega h)}{\omega \sin(\omega h)} \Big(f(x_0, y_0) + f(x_1, y_1) \Big). \tag{2.2}$$

Taylor expansion yields that the local truncation error is $(y^{(3)} + \omega^2 y')h^3/12$. Therefore, the scheme is convergent with order 2. If ω is chosen such that $y^{(3)} + \omega^2 y' = 0$, then the scheme will be convergent with order 3 [12]. Under the segmentation with equidistant points, we apply exponentially fitted trapezoidal (abbreviated to EFT) scheme to (1.1) and get the following formula

$$u_{k+1} = u_k + \frac{1-\cos(\omega h)}{\omega \sin(\omega h)}(v_{k+1} + v_k), \tag{2.3a}$$

$$v_{k+1} = v_k - \frac{1-\cos(\omega h)}{\omega \sin(\omega h)}(u_{k+1} + u_k) + 2\lambda\frac{1-\cos(\omega h)}{\omega h \sin(\omega h)}\Delta W_k, \tag{2.3b}$$

where h is temporal step-size and ω is undetermined. And the numerical values of $u(t_k)$ and $v(t_k)$ are denoted by u_k and v_k, respectively.

Theorem 2.1. *To the linear stochastic system* (1.1), *the EFT scheme* (2.3) *is convergent with root mean-square order* 1.

Proof. To the linear stochastic system (1.1), Euler-Maruyama scheme is convergent with root mean-square order 1 and its formula is

$$\bar{u}_{k+1} = \bar{u}_k + h\bar{v}_k, \tag{2.4a}$$

$$\bar{v}_{k+1} = \bar{v}_k - h\bar{u}_k + \lambda\Delta W_k. \tag{2.4b}$$

Now we let $\bar{u}_k = u_k, \bar{v}_k = v_k$, and consider the local truncation error of the two schemes (2.3) and (2.4). From the EFT scheme (2.3), we get that

$$u_{k+1} = \frac{1}{1+a^2}[(1-a^2)u_k + 2av_k] + \frac{2a^2\lambda}{h(1+a^2)}\Delta W_k, \tag{2.5a}$$

$$v_{k+1} = \frac{1}{1+a^2}[(1-a^2)v_k - 2au_k] + \frac{2a\lambda}{h(1+a^2)}\Delta W_k, \tag{2.5b}$$

where $a = \frac{1-\cos(\omega h)}{\omega \sin(\omega h)}$. Then with (2.4), we obtain the following errors

$$u_{k+1} - \bar{u}_{k+1} = \left(\frac{1-a^2}{1+a^2} - 1\right)u_k + \left(\frac{2a}{1+a^2} - h\right)v_k + \frac{2a^2\lambda}{h(1+a^2)}\Delta W_k, \tag{2.6a}$$

$$v_{k+1} - \bar{v}_{k+1} = \left(\frac{1-a^2}{1+a^2} - 1\right)v_k - \left(\frac{2a}{1+a^2} - h\right)u_k + \lambda(\frac{2a}{h(1+a^2)} - 1)\Delta W_k. \tag{2.6b}$$

Denote $X_k = (u_k, v_k)^T, \bar{X}_k = (\bar{u}_k, \bar{v}_k)^T$. From (2.6), we can derive

$$|E(X_{k+1} - \bar{X}_{k+1})|^2 = \left[\left(\frac{1-a^2}{1+a^2} - 1\right)^2 + \left(\frac{2a}{1+a^2} - h\right)^2\right][E(u_k^2) + E(v_k^2)], \tag{2.7}$$

$$E(|X_{k+1} - \bar{X}_{k+1}|^2) = |E(X_{k+1} - \bar{X}_{k+1})|^2 + \lambda^2 h\left[\frac{4a^4}{h^2(1+a^2)^2} + \left(\frac{2a}{(1+a^2)h} - 1\right)^2\right]. \tag{2.8}$$

Taylor expansion yields that

$$a = \frac{h}{2} + \frac{\omega^2}{12}h^3 + O(h^5), \quad \frac{1-a^2}{1+a^2} - 1 = \frac{-2a^2}{1+a^2} = -\frac{h^2}{2} + \left(\frac{1}{4} - \frac{\omega^2}{12}\right)h^4 + O(h^6), \tag{2.9}$$

$$\frac{2a}{1+a^2} - h = \left(-\frac{1}{4} + \frac{\omega^2}{12}\right)h^3 + O(h^5), \quad \frac{2a}{(1+a^2)h} - 1 = \left(-\frac{1}{4} + \frac{\omega^2}{12}\right)h^2 + O(h^4). \tag{2.10}$$

From (2.7)-(2.10), we obtain that

$$|E(X_{k+1}-\bar{X}_{k+1})|^2 = [E(u_k^2)+E(v_k^2)]\left(\frac{h^4}{4}+\frac{h^6}{144}(\omega^2-3)(\omega^2+9)+O(h^8)\right), \tag{2.11}$$

$$\begin{aligned} E(|X_{k+1}-\bar{X}_{k+1}|^2) &= |E(X_{k+1}-\bar{X}_{k+1})|^2+\lambda^2\frac{h^3}{4}+\lambda^2\frac{h^5}{144}(\omega^2-3)(\omega^2+9)+O(h^7) \\ &= \lambda^2\frac{h^3}{4}+\frac{h^4}{4}[E(u_k^2)+E(v_k^2)]+O(h^5). \end{aligned} \tag{2.12}$$

Then, (2.11) and (2.12) tell us that $E(|X_{k+1}-\bar{X}_{k+1}|^2)=O(h^3)$. So the EFT scheme (2.3) is convergent with root mean-square order 1. □

3. Numerical Analysis of the EFT Scheme

First we consider whether the EFT scheme can preserve the discrete symplectic 2-form [2] of the system (1.1). From (2.5), by direct computation of $du_k\wedge dv_k$, we can derive that

$$du_{k+1}\wedge dv_{k+1} = \frac{1}{(1+a^2)^2}[(1-a^2)du_k+2adv_k]\wedge[(1-a^2)dv_k-2adu_k].$$

Since $du_k\wedge du_k = dv_k\wedge dv_k = 0, du_k\wedge dv_k = -dv_k\wedge du_k$, the equality above implies that $du_{k+1}\wedge dv_{k+1} = du_k\wedge dv_k$. So the EFT scheme is symplectic.

Second we consider whether the numerical solution u_k of the EFT scheme to the system (1.1) can oscillate infinitely many times. From (2.5), we can get that

$$u_k = \frac{1}{1+a^2}[(1-a^2)u_{k-1}+2av_{k-1}]+\frac{2a^2\lambda}{h(1+a^2)}\Delta W_{k-1}, \tag{3.1}$$

$$v_k = \frac{1}{1+a^2}[(1-a^2)v_{k-1}-2au_{k-1}]+\frac{2a\lambda}{h(1+a^2)}\Delta W_{k-1}. \tag{3.2}$$

The formula (3.1) yields that

$$v_{k-1} = \frac{1+a^2}{2a}u_k-\frac{1-a^2}{2a}u_{k-1}-\frac{a\lambda}{h}\Delta W_{k-1}. \tag{3.3}$$

Therefore, with (3.1) and (3.3), we obtain that

$$v_k = \frac{1-a^2}{2a}u_k-\frac{1+a^2}{2a}u_{k-1}+\frac{a\lambda}{h}\Delta W_{k-1}. \tag{3.4}$$

Thus, with (3.4) and (2.5), we derive that

$$u_{k+1} = bu_k-u_{k-1}+s_k, \qquad b = 2\frac{1-a^2}{1+a^2}, \qquad s_k = \frac{2a^2\lambda}{h(1+a^2)}[\Delta W_k+\Delta W_{k-1}]. \tag{3.5}$$

With the notations $Y_k = (u_{k+1},u_k)^T,\ \bar{s}_k = (s_k,0)^T$ and

$$A = \begin{pmatrix} b & -1 \\ 1 & 0 \end{pmatrix}, \tag{3.6}$$

we can derive that

$$Y_k = AY_{k-1}\bar{s}_k = A^kY_0 + A^{k-1}\bar{s}_1 + A^{k-2}\bar{s}_2 + \cdots + A\bar{s}_{k-1} + \bar{s}_k. \tag{3.7}$$

For any positive integer n, denote

$$A^n = \begin{pmatrix} a_n & b_n \\ c_n & d_n \end{pmatrix}.$$

From (3.7), we can get that

$$u_{k+1} = b_k + a_ku_1 + a_{k-1}s_1 + \cdots + a_1s_{k-1} + s_k = b_k + \frac{1}{2}a_kb + \phi_k, \tag{3.8}$$

$$\phi_k = \frac{2a^2a_k\lambda}{(1+a^2)h}\Delta W_0 + \sum_{j=1}^{k} a_{k-j}s_j, \tag{3.9}$$

where $a_0 = 1$. From (3.6), the eigenvalues ρ of (3.6) satisfy that $\rho^2 - b\rho + 1 = 0$. With the expression of b, the eigenvalues are conjugate complex numbers, and they have unit modulus. Suppose that the eigenvalues of A are $\rho_1 = e^{i\theta},\ \rho_2 = e^{-i\theta}$. According to the equation for the eigenvalues of (3.6), According to [4], we get that the corresponding eigenvectors are $(\rho_1, 1)^T, (\rho_2, 1)^T$ and

$$\begin{aligned} A^n &= \begin{pmatrix} \rho_1 & \rho_2 \\ 1 & 1 \end{pmatrix} \begin{pmatrix} \rho_1^n & 0 \\ 0 & \rho_2^n \end{pmatrix} \begin{pmatrix} \rho_1 & \rho_2 \\ 1 & 1 \end{pmatrix}^{-1} \\ &= \frac{1}{\rho_1 - \rho_2} \begin{pmatrix} \rho_1^{n+1} - \rho_2^{n+1} & \rho_2^n - \rho_1^n \\ \rho_1^n - \rho_2^n & \rho_2^{n-1} - \rho_1^{n-1} \end{pmatrix}. \end{aligned}$$

Therefore

$$\begin{aligned} b_k + \frac{1}{2}a_kb &= \frac{1}{\rho_1 - \rho_2}\left[\rho_2^k - \rho_1^k + \frac{b}{2}(\rho_1^{k+1} - \rho_2^{k+1})\right] \\ &= \frac{1}{\sin\theta}\left[-\sin k\theta + \frac{b}{2}\sin(k+1)\theta\right]. \end{aligned} \tag{3.10}$$

From (3.10), $b_k + \frac{1}{2}a_kb$ is bounded. For ϕ_k, from (3.5), we can derive that

$$\begin{aligned} \phi_k &= \frac{2a^2a_k\lambda}{(1+a^2)h}\Delta W_0 + \sum_{j=1}^{k} \frac{2a^2\lambda}{h(1+a^2)} a_{k-j}[\Delta W_j + \Delta W_{j-1}] \\ &= \frac{2a^2a_k\lambda}{(1+a^2)h}\Delta W_0 + \sum_{j=0}^{k-1} \frac{2a^2\lambda}{(1+a^2)h} a_j\Delta W_{k-j} + \sum_{j=1}^{k} \frac{2a^2\lambda}{(1+a^2)h} a_{j-1}\Delta W_{k-j} \\ &= \sum_{j=1}^{k} \mu_j\Delta W_{k-j}, \end{aligned} \tag{3.11}$$

where

$$\begin{aligned}
\mu_0 &= \frac{2a^2\lambda}{(1+a^2)h},\\
\mu_j &= \frac{2a^2\lambda}{(1+a^2)h}\,(a_j + a_{j-1})\\
&= \frac{2a^2\lambda}{(1+a^2)h}\frac{1}{\rho_1-\rho_2}\left(\rho_1^{j+1} - \rho_2^{j+1} + (\rho_1^j - \rho_2^j)\right)\\
&= \frac{2a^2\lambda}{(1+a^2)h\sin\theta}\Big(\sin(j+1)\theta + \sin j\theta\Big)\\
&= \frac{4a^2\lambda}{(1+a^2)h\sin\theta}\cos\frac{\theta}{2}\sin\left(j+\frac{1}{2}\right)\theta, \quad j = 1,\dots,k. \qquad (3.12)
\end{aligned}$$

Therefore $\phi_k \sim N(0, h\sum_{j=0}^{k}\mu_j^2)$. From (2.9) and (3.12), μ_j is bounded. Clearly, $\lim_{j\to\infty}\sin(j+\frac{1}{2})\theta \neq 0$. Then $\lim_{j\to\infty}\mu_j \neq 0$. Thus

$$\lim_{k\to\infty} h\sum_{j=0}^{k}\mu_j^2 = \infty.$$

According to the Law of the Iterated Logarithm ([3,4]), for sufficiently large k and arbitrary $\varepsilon \in (0,\ 1)$, ϕ_k will infinitely often oscillate beyond the bound

$$(1-\varepsilon)\sqrt{2h\sum_{j=0}^{k}\mu_j^2 \ln\ln\left(h\sum_{j=0}^{k}\mu_j^2\right)}$$

almost surely. From (3.8) and (3.10), we can see that u_k behaves similarly.

Third, we consider whether the discrete second moment $E(u_k^2 + v_k^2)$ of the EFT scheme to the system (1.1) can grow linearly with time. From the EFT scheme (2.5), we derive that

$$u_{k+1}^2 + v_{k+1}^2 = u_k^2 + v_k^2 + \frac{4a^2\lambda^2}{(1+a^2)h^2}\Delta W_k^2 + \frac{4a\lambda}{(1+a^2)h}(v_k - au_k)\Delta W_k. \qquad (3.13)$$

Therefore, we get that

$$E(u_{k+1}^2 + v_{k+1}^2) = E(u_k^2 + v_k^2) + \lambda^2 h\frac{4a^2}{(1+a^2)h^2}. \qquad (3.14)$$

Taylor expansion (2.9) yields that

$$\begin{aligned}
&\frac{4a^2}{(1+a^2)h^2} = 1 + \frac{\omega^2-3}{6}h^2 + O(h^4),\\
&E(u_{k+1}^2 + v_{k+1}^2) = E(u_k^2 + v_k^2) + \lambda^2 h\left[1 + \frac{\omega^2-3}{6}h^2 + O(h^4)\right].
\end{aligned}$$

With initial condition of system (1.1), this indicate that

$$E(u_k^2 + v_k^2) = 1 + \lambda^2 t_k + \frac{\omega^2-3}{6}\lambda^2 t_k h^2 + O(t_k h^4). \qquad (3.15)$$

Theorem 3.1. *To the system* (1.1)*, the EFT scheme is symplectic. Its numerical solution* u_k *oscillates infinitely many times. Moreover its discrete second moment* $E(u_k^2+v_k^2)$ *grows linearly with time approximately.*

Note that from Eq. (3.13) for the deterministic system (1.1) with $\lambda = 0$, the numerical solutions satisfy that $u_k^2 + v_k^2 = 1$. This means that the phase trajectory of the numerical solutions is a circle with radius 1.

4. Numerical Result

Now we apply above EFT scheme to solve the stochastic oscillator system (1.1) and test the behavior of the scheme. According to theorem 1, the choice of ω does not affect the convergence order of EFT scheme in the stochastic case. According to the derivation of exponentially fitted trapezoidal scheme in [18], EFT scheme is exact with $\omega = 1$ for deterministic system (1.1) with $\lambda = 0$. For $\lambda \neq 0$, the stochastic case is complicated and we choose different ω in the experiment.

In the deterministic case with $\lambda = 0$, we apply EFT scheme with $\omega = 1, h = 0.1$. In Figure 4.1, we depict the phase trajectory of the numerical solutions for $t \in (0,\ 1000]$. In Figure 4.2, we depict the corresponding numerical errors

$|u_k - u(t_k)|$, which increase with time due to the computer rounding error.

In the stochastic case with $\lambda \neq 0$, we simulate the theoretical solutions (1.2) with step size 2^{-14}. To implement the EFT scheme, we first apply $\omega = 1,\ \lambda = 0.1$ and different step sizes h. Figure 4.3 displays the convergence order of EFT scheme at $T = 1$. The errors are obtained by the sample average of mean square error of 500 numerical solutions and theoretical solutions. Denote the exact and numerical solution under the kth $W(t)$ sample by $u^k(t_n)$ and u_n^k. Then the errors are defined by

$$e_n = \sqrt{\frac{1}{500}\sum_{k=1}^{500}(u^k(t_n) - u_n^k)^2}.$$

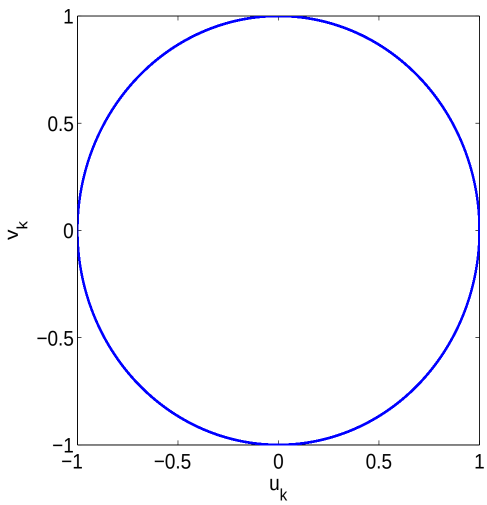

Fig. 4.1. Phase trajectory of numerical solutions with EFT scheme.

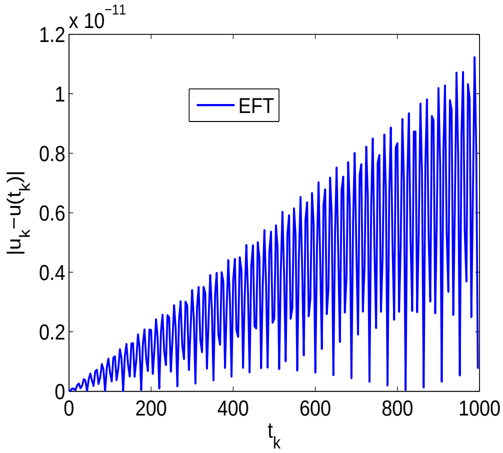

Fig. 4.2. Errors of the numerical solutions with EFT scheme.

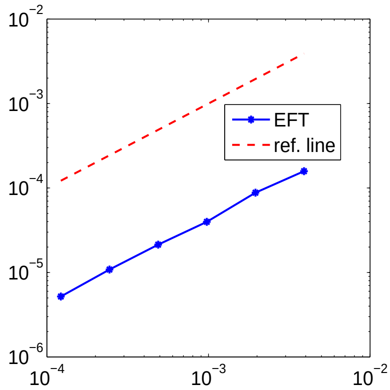

Fig. 4.3. Order test of EFT scheme with $\omega = 1, \lambda = 0.1, T = 1$.

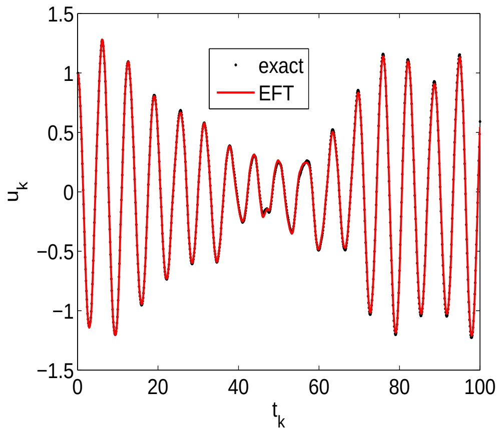

Fig. 4.4. Oscillation of theoretical solutions and numerical solutions with EFT scheme.

In Figure 4.3, the errors versus decreasing step sizes are depicted in log-log scale. The reference line has slope 1. It confirms that the EFT scheme is convergent with root mean-square order1.

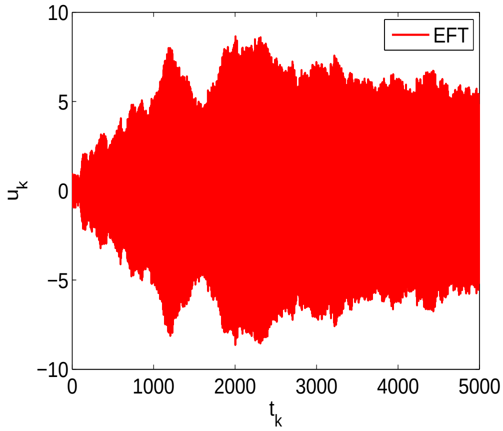

Fig. 4.5. Oscillation of the numerical solutions with EFT scheme.

We choose $\omega = 0.75, \lambda = 0.1, h = 0.1$ next. In Figure 4.4, we plot time evolution trajectory of $u(t)$ for one sample of numerical solution and theoretical solution under the same $W(t)$ sample for $t \in (0,\ 100]$. We can see that the numerical solutions simulate approximately the oscillation of theoretical solutions. In Figure 4.5, we plot time evolution trajectory of $u(t)$ for one sample of numerical solution for $t \in (0,\ 5000]$. It confirms that the simulation of oscillation with long time is stable.

We choose $\omega = 0.9, \lambda = 0.2, h = 0.1$ below. In Figure 4.6, we depict time evolution trajectory of $u(t)$ for the sample average of 10^4 numerical solutions for $t \in (0,\ 5000]$. The reference line with slope 1 denotes the second moment of theoretical solutions. The figure shows that the numerical second moment $E(u_k^2) + E(v_k^2)$ grows linearly with time approximately.

At last, we compare EFT scheme with the midpoint rule in [3]

$$u_{n+1} = u_n + \frac{h}{2}(v_{n+1} + v_n),\ \ v_{n+1} = v_n - \frac{h}{2}(u_{n+1} + u_n) + \lambda \Delta W_n,$$

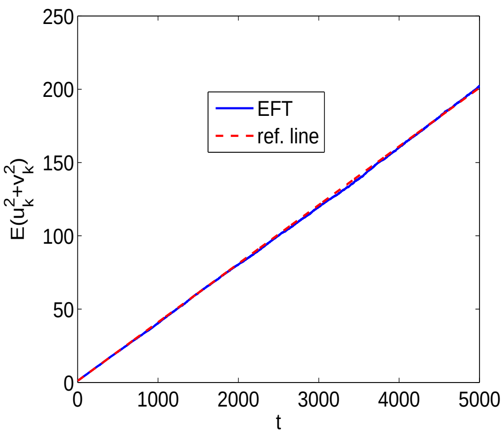

Fig. 4.6. Approximate preservation of the linear growth property with EFT scheme.

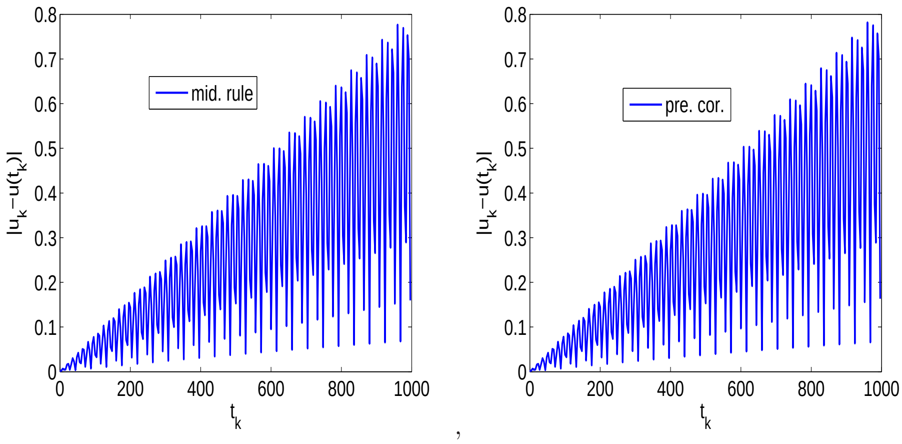

Fig. 4.7. Errors of the numerical solutions for the midpoint rule (left) and predictor-corrector method (right) with $\lambda = 0, h = 0.1$.

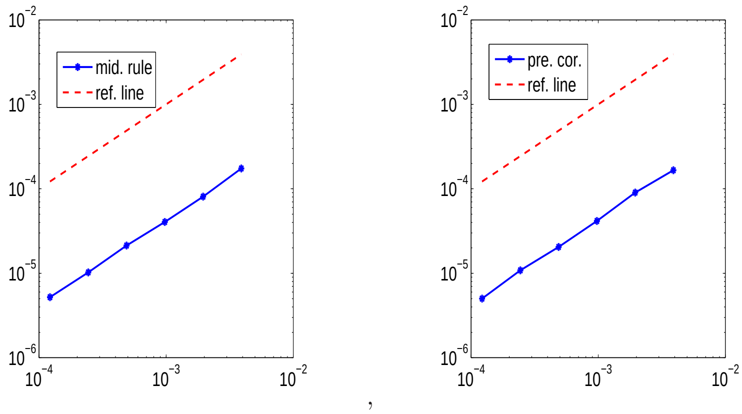

Fig. 4.8. Order test for the midpoint rule (left), predictor-corrector method (right) with $\lambda = 0.1, h = 0.1, T = 1$.

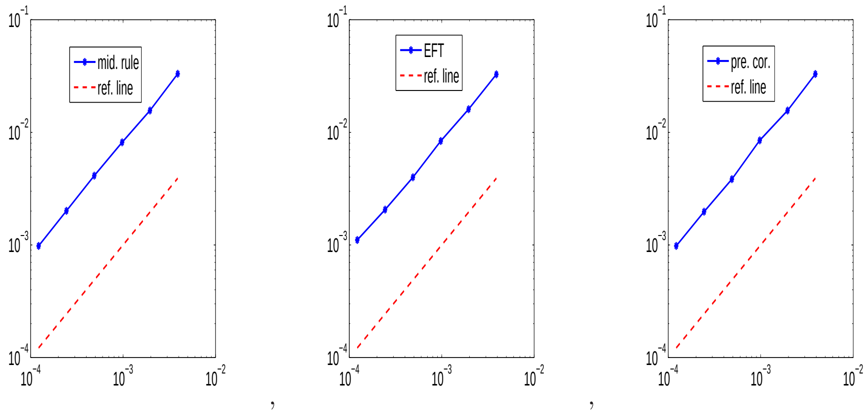

Fig. 4.9. Order test for the midpoint rule (left), EFT scheme (middle) and predictor-corrector method (right) with $\omega = 1, \lambda = 20, h = 0.1, T = 1$.

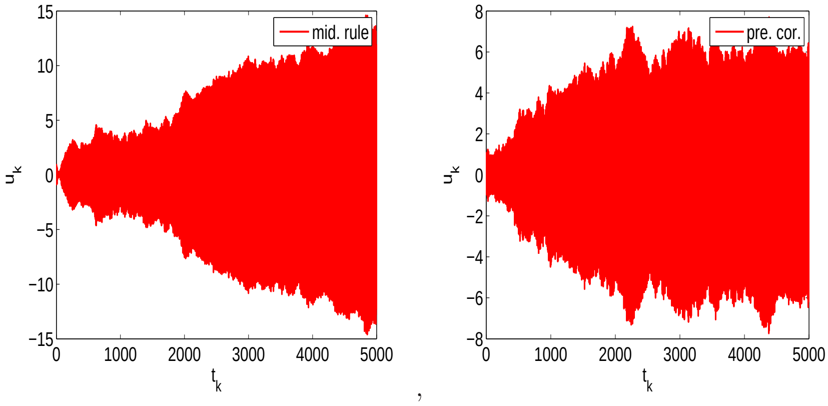

Fig. 4.10. Oscillation of the numerical solutions for the midpoint rule (left) and predictor-corrector method (right) with $\lambda = 0.1, h = 0.1$.

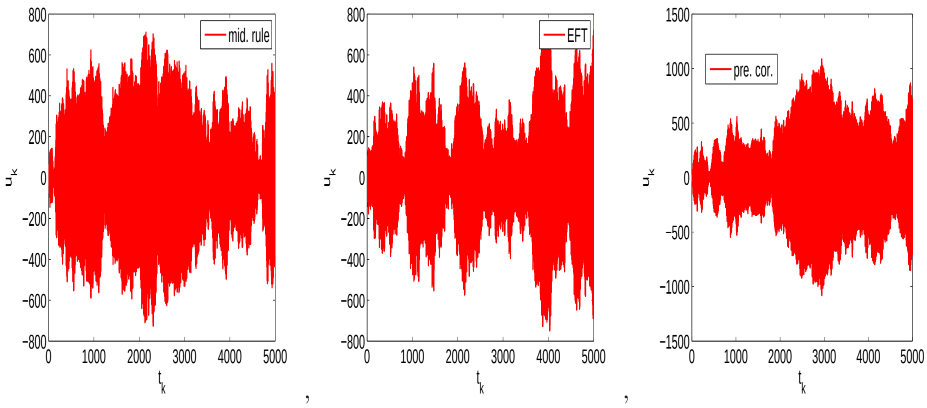

Fig. 4.11. Oscillation of the numerical solutions for the midpoint rule (left), EFT scheme (middle) and predictor-corrector method (right) with $\omega = 0.75, \lambda = 20, h = 0.1$.

and the predictor-corrector method with $k = 2$ in [4]

$$u_{n+1} = \left(1 - \frac{h^2}{2}\right)u_n + h\left(1 - \frac{h^2}{4}\right)v_n + \frac{\lambda h}{2}\Delta W_n,$$

$$v_{n+1} = -h\left(1 - \frac{h^2}{4}\right)u_n + \left(1 - \frac{h^2}{2} + \frac{h^4}{4}\right)v_n + \lambda\left(1 - \frac{h^2}{4}\right)\Delta W_n.$$

The data used for the midpoint rule and predictor-corrector method are the same as for EFT scheme.

From Figures 4.2 and 4.7, we find that in the deterministic case, the EFT scheme has smaller errors than the midpoint rule and predictor-corrector method. While in the stochastic case, the numerical errors for these three schemes have the same order of the magnitude (see Figures 4.3, 4.8 and 4.9). From Figures 4.5, 4.10 and 4.11, the three schemes preserve the behavior of oscillation with long time for numerical solutions approximately. From Figures 4.6, 4.12 and 4.13, the three schemes preserve the linear growth property with the numerical solutions approximately.

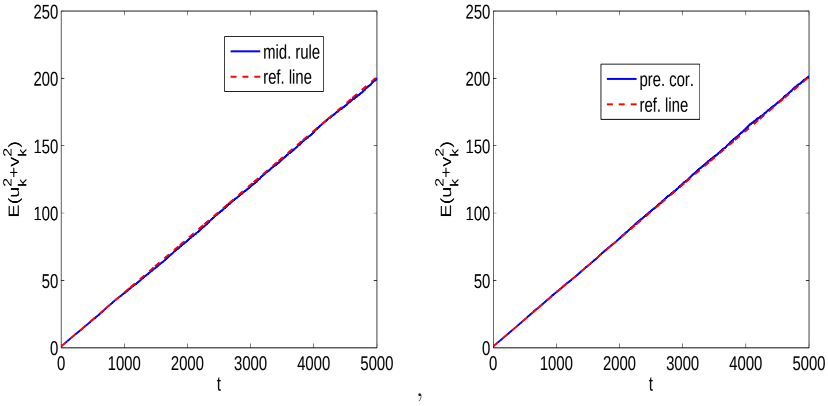

Fig. 4.12. Approximate preservation of the linear growth property with the numerical solutions for the midpoint rule (left) and predictor-corrector method (right) with $\lambda = 0.2, h = 0.1$.

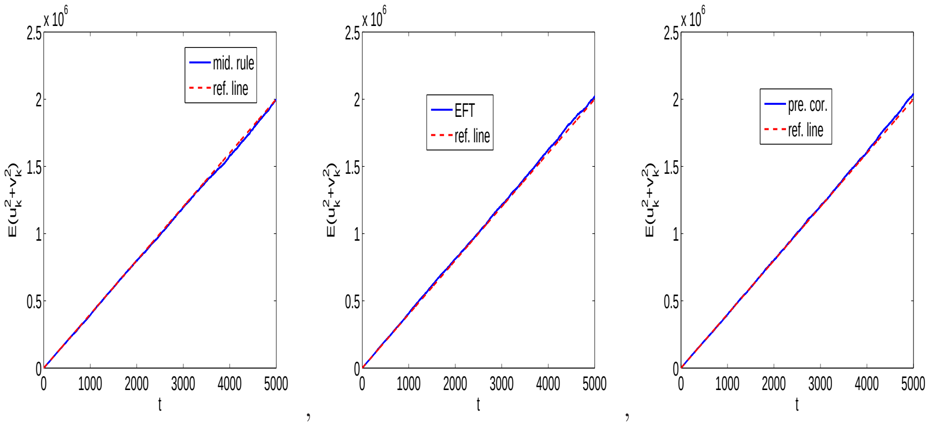

Fig. 4.13. Approximate preservation of the linear growth property with the numerical solutions for the midpoint rule (left), EFT scheme (middle) and predictor-corrector method (right) with $\omega = 0.9, \lambda = 20, h = 0.1$.

5. Conclusion

Exponentially fitted trapezoidal scheme (4) is applied to linear stochastic oscillator system (1) and generates symplectic EFT scheme (5). In deterministic case, the EFT scheme is exact with $\omega = 1$. In the stochastic case, the EFT scheme is convergent with root mean-square order 1 with arbitrary ω. The behavior of oscillation with long time for the numerical solutions is preserved. EFT scheme preserves the linear growth property of the solutions approximately.

It may be worthwhile to generalize the exponential fitted schemes to stochastic differential equations with oscillating solutions. The generalization of the symplectic exponential fitted schemes to stochastic Hamiltonian systems with oscillating solutions may be also valuable. Further discussion and research about the generalization will be needed.

Acknowledgements. This work is supported by National Natural Science Foundation of China (Grant Nos. 11501082, 11571128), Natural Science Foundation of Shandong Province(Nos. ZR2015AL016, ZR2016AQ07) and Project of Shandong Province Higher Educational Science and Technology Program (No J17KA156). The authors wish to thank the reviewers for valuable comments.

References

[1] X. Mao, Stochastic Differential Equations and Applications. Horwood, Chichester, 1997.

[2] G. Milstein, Y. Repin, M. Tretyakov, Numerical methods for stochastic systems preserving symplectic structure, *SIAM J. Numer. Anal.*, **40**:4 (2002), 1583-1604.

[3] A. Melbø, D. Higham, Numerical simulation of a linear stochasctic oscillator with additive noise, *Appl. Numer. Math.*, **51**:1 (2004), 89-99.

[4] J. Hong, R. Scherer, L. Wang, Predictor-corrector methods for a linear stochastic oscillator with additive noise, *Math. Comput. Model.*, **46**:5 (2007), 738-764.

[5] X. Lu, Symplectic schemes for quasilinear wave equations of Klein-Gordon and Sine-Gordon type, *J. Comput. Math.*, **19**:5 (2001), 475-488.

[6] L. Huang, P. Zeng, A new multi-symplectic scheme for nonlinear "good" Boussinesq equation, *J. Comput. Math.*, **21**:6 (2003), 703-714.

[7] J. Chen, M. Zhao, Multi-symplectic Fourier pseudo-spectral method for the nonlinear Schrödinger equation, *Electron T. Numer. Ana.*, **12** (2001), 193-204.

[8] J. Hong, L. Kong, Novel multi-symplectic integrators for nonlinear fourth-order Schrödinger equation with trapped term, *Commun. Comput. Phys.*, **7** (2010), 613-630.

[9] J. Hong, X. Liu, C. Li, Multi-symplectic Runge-Kutta-Nyström methods for nonlinear Schrödinger equations with variable coefficients, *J. Comput. Phys.*, **226** (2007), 1968-1984.

[10] L. Kong, J. Hong, L. Wang, F. Fang, Symplectic integrator for nonlinear high order Schrödinger equation with a trapped term, *J. Comput. Appl. Math.*, **231** (2009), 664-679.

[11] G. Vanden Berghe, H. De Meyer, et al. Exponentially-fitted Runge-Kutta methods, *J. Comput. Appl. Math.*, **125** (2000), 107-115.

[12] G. Vanden Berghe, L.Gr. Ixaru, H. De Meyer, Frequency determination and step-length control for exponentially- fitted Runge-Kutta methods, *J. Comput. Appl. Math.*, **132** (2001), 95-105.

[13] T. Simos, Exponentially-fitted Runge-Kutta-Nyström method for the numerical solution of initial-value problems with oscillating solutions, *Appl. Math. Lett.*, **15**:2 (2002), 217-225.

[14] G. Vanden Berghe, M. Van Daele, et al. Exponentially-fitted Runge-Kutta methods of collocation type: fixed or variable knot points, *J. Comput. Appl. Math.*, **159** 2003, 217-239.

[15] J. Vigo-Aguiar, T.E. Simos, A. Tocino, An adapted symplectic integrator for Hamiltonian systems, *Int. J. Mod. Phys. C*, **12** (2001), 225-234.

[16] H. Van de Vyver, A symplectic exponentially fitted modified Runge-Kutta-Nyström method for the numerical integration of orbital problems, *New Astronomy*, **10** (2005), 261-269.

[17] H. Van de Vyver, A fourth-order symplectic exponentially fitted integrator, *Comput. Phys. Commun.*, **174** (2006), 255-262

[18] M. Calvo, J. Franco, J. Montijano, et al. Structure preservation of exponentially fitted Runge-Kutta methods, *J. Comput. Appl. Math.*, **218** (2008), 421-434.